

THE BEAGLE 2 LANDING SITE IN ISIDIS PLANITIA J. C. Bridges¹, A. M. Seabrook^{2,3}, J. R. Kim⁴, J-P. Muller⁴, D. A. Rothery³, C. T. Pillinger², M. R. Sims⁵, I. P. Wright², M. M. Grady¹, K. L. Mitchell^{4,6}, J. G. Morley⁴
¹Dept. of Mineralogy, Natural History Museum, Cromwell Road, London SW7 5BD, UK, (j.bridges@nhm.ac.uk),
²PSSRI, Open University, Milton Keynes MK7 6AA, UK, ³ Dept. of Earth Sciences, Open University, Milton Keynes, UK, ⁴Dept. of Geomatic Engineering, University College London, Gower St., WC1E 6BT, UK, ⁵ Dept. of Physics and Astronomy, University of Leicester, Leicester, UK, ⁶ Environmental Science Dept., Lancaster University, Lancaster LA1 4YQ, UK.

Introduction: The Mars landing site for Beagle 2 [1] lies within the Isidis Planitia basin. This site was chosen because it satisfies the engineering constraints for landing and operations [2] together with being an area with geological characteristics that suggest it is suitable for the exobiological, atmospheric and chemical analyses that Beagle is designed for.

Here we summarise the MOLA, MOC, thermal inertia and other data gathered on the scale of the landing ellipse. A regional perspective is given in [3,4]. From the data it is suggested that Isidis has preserved evidence for phreatic activity after the deposition of volatile-rich smooth plains material over an underlying mare-like basement.

The MDIM co-ordinates of the centre of the landing ellipse are 270°W, 10.6°N. Ellipse size and orientation depends on the flight path angle (15-18°), the exact figure will not be known until close to launch in June 2003. Landing occurs in January 2004 during martian early spring ($L_s = 322^\circ$ to 53° , lifetime 180 martian days). The largest 3 sigma probability landing ellipse, corresponding to a flight path angle of 15°, has dimensions of 495 x 95 km in a 77.6°, clockwise from north, orientation.

Topography and structure: Within this ellipse, the ground surface slopes from NE to SW, with a drop in elevation from -3600 to -3900 m. (-2 km relative to pressure datum). A 1/64th gridded DEM was constructed from MOLA track data using kriging interpolation after deletion of noisy track data [5]. Slope angle distributions across the landing area were calculated for 0.25 km, N-S and 2.5 km, E-W MOLA baselines. These baselines both gave average slope values of 0°.

The Isidis basin is underlain by a lunar mare-like structure [3,4]. The linear topographic highs identified by MOLA data are analogous to lunar wrinkle ridges. These are the most pronounced topographic features (on scales > km) across the plain. An example of the buried ridges is shown (Fig. 1a,b) in a WNW-ESE trending area of relatively high relief which is 100 m above the surrounding plain. The slopes associated with this rise are mostly < 6°. Their subdued morphology is a result of partial burial underneath the Amazonian smooth plains deposits (Aps) and Hesperian Ridged member of the Vastitas Borealis formation (Hvr).

nian smooth plains deposits (Aps) and Hesperian Ridged member of the Vastitas Borealis formation (Hvr).

Isidis landforms: Sub-km diameter cones with summit pits are found singly or along chains across Isidis [6,7]. MOC images show that these landforms cover ~5 % of Isidis (Figure 2). In contrast to a field of scattered cones in Amazonis Planitia described in [8], these are not superimposed on obvious lava-flow-like features, but sit directly on the smooth plains deposits, which on MOC images can be seen to have abundant impact craters in the <500 m size range and 9 impact craters ≥ 3 km diameter within the area of the landing ellipse. The Isidis cones and cone chains are clearly younger than the surface on which they sit (they do not show signs of the impact cratering seen in the surrounding plains). Therefore it is by no means clear that the Isidis cones are rootless craters ('pseudocraters') generated by escape of subsurface volatiles triggered by heat from emplacement of lava flows, which is the preferred explanation in Amazonis [8]. They are probably either genuine volcanic cinder cones or else pseudocraters generated by a subsurface heating or possibly decompression mechanism.

It is likely that hydrothermal activity associated with the phreatic or decompression volatile release has taken place and Beagle's analyses will help characterise that. No clear association between the cones and the pattern of buried wrinkle ridges [3,4] in the underlying basement is seen.

The smooth plains material is likely to be the source of the volatiles, although whether it was deposited through a mass flow of debris/mud [7] or air-fall [6] remains to be determined.

Thermal inertia and rock abundances: Uninterpolated MGS thermal inertia (TI) data from [9,10] has been used to construct a map of Isidis at a resolution of 8 pixels per degree. This shows that the lowest values < 250 $\text{Jm}^{-2}\text{s}^{-0.5}\text{K}^{-1}$ are found to the north and west of the basin, most of the basin interior, including across the landing ellipse is 300-400 $\text{Jm}^{-2}\text{s}^{-0.5}\text{K}^{-1}$. The highest values > 500 $\text{Jm}^{-2}\text{s}^{-0.5}\text{K}^{-1}$ are found at the southern part of the basin, suggesting that this part of Isidis may be

prohibitively rocky. The Mars average TI is $250 \text{ Jm}^{-2}\text{s}^{-0.5}\text{K}^{-1}$ [9].

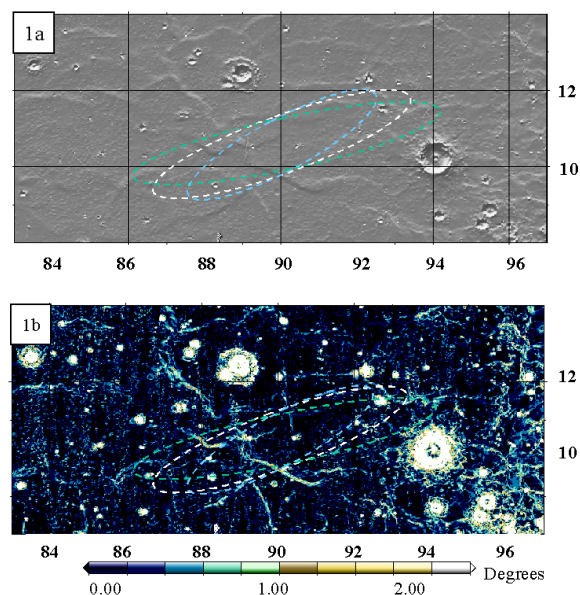


Figure 1. (a) Shaded relief map constructed from MOLA data [5]. (b) Slope map constructed from N-S and E-W MOLA baselines. 3-sigma landing ellipses for flight path angles of 15° , 18° and 20° are shown in green, white and blue. Aerocentric co-ordinates.

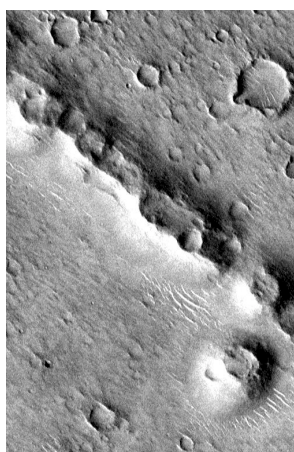


Figure 2. Cone chain in Isidis (part of MOC ab 103405), 2.6 km across. The MOC image is in mirrored orientation and centred on 16.8°N , 276.0°W . A landing ellipse position was chosen that has similar landforms to those shown here but with a lower areal coverage. Small-scale dunes are situated near the gap in the cone chain and beside the isolated cone in the southeast.

The fairly high albedo of Isidis ~ 0.25 - 0.27 coupled with the moderate/high thermal inertia values is consistent with thin coating of dust over a rock or duricrust-bearing substrate. The rock abundances [11] across the landing ellipse vary between 5-15 %, although some areas of higher and lower abundance do occur. The TI/albedo characteristics of Isidis are most similar to the 'Unit C' division of the martian surface [9], although the TI of Isidis is higher than the typical range for that mapped unit. The dust veneer and distribution of rocks/duricrusts in the upper few cm of soil in Isidis may be similar to the Chryse land surface.

MOC images show the presence of some aeolian activity. Dune fields are localised within some of the craters and around a minority of the pitted hills. Discontinuous, high albedo features aligned along a predominantly NW-SE orientation are probably isolated dunes or drifts. These are common in the MOC images and suggest that the overprint of aeolian activity in Isidis may be similar to that of the Viking 1 landing area. Astronomical records [12] do not show the main part of the Isidis basin to be particularly associated with regional dust storms.

Summary: Isidis Planitia is covered by volatile-rich plains deposits. Volatile release from the subsoil has created sub-km size conical landforms. The soil and rock chemistry and mineralogy will probably reflect this process and, together with the evidence for regional volatile enrichment, this suggests a suitable environment for Beagle 2 which is designed to detect H_2O and organic matter. Digital elevation modelling of the region around the Beagle 2 landing site (centre 270°W , 10.6°N) shows that the elevation varies by 300 m over 500 km distance and has few slopes that exceed 6° . The most prominent topographic features are subdued ridges which rise ≤ 200 m above the surrounding plain and stretch for hundreds of km. These are surface manifestations of wrinkle ridges in the basement underlying the later plains deposits.

References: [1] www.beagle2.com [2] Bridges J. C. et al. (2000) *Meteorit. and Planet. Sci.* 35, A34. [3] Head J. W. et al. (2001) *JGR*, in review. [4] Head J. W. and Bridges J. C. (2001) *LPS XXXII*. [5] Kim J. R. et al. (2001) *LPS XXXII*; Kim J. R. et al. (2000) *ISPRS 2000 Proc.*, (CD-Rom). [6] Grizzaffi P. and Schultz P. (1989) *Icarus*, 77, 358-381. [7] Tanaka K. L. et al. (2000) *LPS XXXI*, #2023. [8] Fagents S. A., and Greeley R. *AGU Fall*, 2000. [9] Mellon M. T. et al. (2000) *Icarus* (in press). [10] <http://argyre.colorado.edu/inertia/> [11] Christensen P.R. (1986) *Icarus*, 68, 217-238. [12] Martin L. J. and Zurek R. W. (1993) *JGR*, 98, 3221-3246.